Science of the Total Environment 712 (2020) 136453

Contents lists available at ScienceDirect

Science of the Total Environment

journal homepage: www.elsevier.com/locate/scitotenv

Integration of proteomics and metabolomics reveals promotion of proliferation by exposure of bisphenol S in human breast epithelial MCF-10A cells

Wei Huang [a,b], Lin Zhu [a], Chao Zhao [a], Xiangfeng Chen [c], Zongwei Cai [a,*]

[a] State Key Laboratory of Environmental and Biological Analysis, Department of Chemistry, Hong Kong Baptist University, Hong Kong, China
[b] Department of Chemistry and Molecular Sciences, Wuhan University, Wuhan, China
[c] Laboratory for Applied Technology of Sophisticated Analytical Instruments, Shandong Analysis and Test Centre, Qilu University of Technology, Shandong, China

HIGHLIGHTS

- BPS altered the proliferation of MCF-10A cells in a hormetic manner.
- Low dose of BPS promoted proliferation of MCF-10A cells.
- EGFR related pathways were involved in promotion of proliferation by BPS.
- Metabolic pathways were regulated by BPS to sustain cell proliferation.

GRAPHICAL ABSTRACT

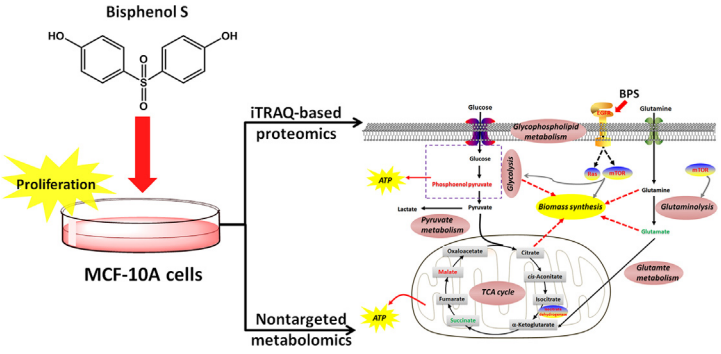

ARTICLE INFO

Article history:
Received 13 October 2019
Received in revised form 30 December 2019
Accepted 30 December 2019
Available online 07 January 2020

Editor: Jay Gan

Keywords:
Bisphenol S
Human breast epithelial cell
Hormetic effect
Proliferation
Proteomics
Metabolomics

ABSTRACT

Bisphenol S (BPS) has been reported to have similar estrogenic effects as bisphenol A (BPA). Considering the endocrine disrupting effects of BPS, in this study, we investigated the effects of BPS exposure on normal human breast epithelial cell line MCF-10A by using mass spectrometry (MS)-based metabolomics and quantitative proteomics. We found that exposure to BPS for 24 h altered the proliferation of MCF-10A cells in a hormetic manner with the highest proliferation rate at the dosage of 1 μM. A total of 200 proteins were identified to be significantly changed by 1 μM of BPS exposure. The upregulation of epidermal growth factor receptor (EGFR) and Ras/mTOR-related proteins implied that EGFR-mediated pathways were involved in BPS-induced proliferation of MCF-10A cells. In addition, several proliferation-related protein markers were found to be elevated, such as MKI67 and CDH1, further indicating the promotion of proliferation by low dose of BPS exposure. Besides, 35 endogenous metabolites were found to be significantly changed. The joint pathway analysis of the altered metabolites and proteins suggested changes in pathways of tricarboxylic acid (TCA) cycle, purine metabolism, pyruvate metabolism and lipid metabolism, which were involved in sustaining cell proliferation and cellular signal transduction. Taken together, this study provides insights into the effects and the potential mechanisms of BPS on estrogen receptor α-negative normal breast cell line MCF-10A, broadening our knowledge about the risk of using BPS as the alternative of BPA.

* Corresponding author.
E-mail address: zwcai@hkbu.edu.hk (Z. Cai).

https://doi.org/10.1016/j.scitotenv.2019.136453
0048-9697/

1. Introduction

Bisphenol A (BPA) has been reported to have many potential adverse effects on human health, including influence on neuronal development, reproductive toxicity, endocrine disrupting effects, induction of DNA damage, correlation with chronic diseases or even cancer (Rezg et al., 2014). Due to the mounting evidence of harmful effects and public concern, BPA has been gradually banned in consumer products, such as baby bottles, food containers, or even thermal papers (Commission, 2011; Jalal et al., 2018). Structural analogues of BPA including bisphenol S (BPS) are now frequently used as BPA alternatives (Rochester and Bolden, 2015). A strong negative correlation between BPA and BPS levels was found in thermal receipt papers, suggesting that BPS is the primary replacement of BPA in paper products (Liao et al., 2012a). In addition, BPS has been detected in 81% of urine samples from the general populations in the United States and seven Asian countries, illustrating the wide-spread human exposure of this bisphenol analogue (Liao et al., 2012b).

An important concern about BPA is its effects in mammary gland development and progression of breast cancer (Wang et al., 2017). Researchers showed that rodents prenatally exposed to environmentally relevant levels of BPA resulted in an increased risk of developing breast cancer (Ayyanan et al., 2011; Mandrup et al., 2016). BPA could induce proliferation in estrogen receptor α (ERα)-positive breast cells by activation of ER-mediated transcription (Samuelsen et al., 2001). These studies illustrated the estrogenic power of BPA. However, BPA has also been reported to induce proliferation in ERα-negative cells, including MCF-10A cells, by nonestrogenic mechanisms involving upregulation of *c-Myc* and other cell-cycle regulatory proteins (Pfeifer et al., 2015). Besides, in ER negative breast cells which express G protein-coupled receptor (GPER), BPA stimulated the proliferation and migration through GPER/EGFR (epidermal growth factor receptor) transduction pathways (Pupo et al., 2012). These findings suggested that BPA could elicit biological effects in both ER positive and negative breast cells, which might stimulate breast cancer progression.

BPS has the similar chemical structure as BPA. Compared with a large number of studies about BPA, investigation on BPS has remained rather limited. Recent evidence suggested that BPS was as hormonally active as BPA and also able to induce endocrine disrupting effects (Chen et al., 2016). Low dose of BPS exposure during perinatal period altered the mammary gland development in mouse (Kolla et al., 2018; Tucker et al., 2018). BPS also altered the lactating mammary gland and nursing behaviors in exposed female mice (LaPlante et al., 2017). BPS could induce epigenetic and transcriptional changes, promoting cell cycle progression and cell proliferation in ERα-positive MCF-7 breast cancer cells (Huang et al., 2019; Lin et al., 2019; Williams and Darbre, 2019). Although studies on triple-negative breast cancer (TNBC) cells revealed that BPS can promote migration, but not proliferation of TNBC cells (Deng et al., 2018), the effects of BPS exposure on ER-negative normal breast cells were largely unknown. Due to the heterogeneity of cells in rodent mammary gland tissue (Saji et al., 2000), the effects of BPS on normal ER negative breast cells and the related non-estrogenic mechanisms need to be elucidated. Therefore, proper models representing such subtype are desirable. The MCF-10A cell line is a widely used model for its ER negative property and near normal phenotype (Soule et al., 1990). In tissue culture plates, the MCF-10A cells would form dome structures at confluence, making it a model of choice for breast tumor progression studies (Zientek-Targosz et al., 2008). In this study, we assessed the influence induced by BPS exposure on MCF-10A cells.

In the last few decades, with the advancement in mass spectrometry (MS) instrumentation, MS-based proteomics and metabolomics technologies have been widely used to conduct complete assessment of the functional cellular alterations, enabling more profound biological insights into mechanisms of disease pathogenesis, action of drugs, effects of toxic substances, and so on. Thus, by using these techniques, simultaneous characterization of tens to thousands of proteins or metabolites associated with chemical toxicity are achievable in an untargeted manner (Gowda et al., 2008; Gstaiger and Aebersold, 2009; Aebersold and Mann, 2016; Zhang et al., 2016). Integration of proteomics and metabolomics could provide more comprehensive information from different aspects of biological processes. Such approaches have been successfully used in the toxicity assessment of numerous environmental chemicals, such as benzo[*a*]pyrene (BaP) (Chen et al., 2018a), dichlorodiphenyltrichloroethane (DDT) (Song et al., 2017), tetrabromobisphenol A (TBBPA) (Ji et al., 2016), tetrabromodiphenyl ether (BDE-47) (Ji et al., 2013; Ji et al., 2019), heavy metal (Go et al., 2014) and some nanoparticles (Gioria et al., 2016; Xie et al., 2018). Herein, we applied this strategy to examine the changes induced by BPS in pathways from protein level and metabolite level to understand how BPS exerts its effects on the ER-negative MCF-10A cells.

2. Materials and methods

2.1. Materials

Mammary epithelial growth medium (MEGM) was purchased from Lonza Inc. (MD, USA). Bisphenol S (BPS), dimethylsulfoxide (DMSO), formic acid (FA), 4-chloro-phenylalanine (4-Cl-Phe) were obtained from Sigma-Aldrich (St. Louis, USA). Phosphate buffered saline (PBS), trypsin-EDTA (0.25%) and trypsin inhibitor were purchased from Gibco (ThermoFisher Scientific, USA). Cell culture dishes and 96-well plates were obtained from Corning (New York, USA). All solvents were HPLC grade and obtained from Merck (Darmstadt, Germany). Water used throughout this work was purified with a Milli-Q system (Millipore, Billerica, MA, USA) and exhibited a resistivity of 18 on delivery.

2.2. Cell culture

Human mammary epithelial cell line MCF-10A was purchased from the American Type Culture Collection (ATCC). MCF-10A cells were cultured under the ATCC recommended conditions. Briefly, MCF-10A cells were maintained in MEGM medium containing human epidermal growth factor (hEGF) (10 ng/mL), insulin (5 μg/mL), bovine pituitary extract (52 μg/mL), hydrocortisone (0.5 μg/mL), gentamicin sulfate-amphotericin (GA-1000) (50 μg/mL) and cholera toxin (100 ng/mL) under an atmosphere of 5% CO_2 at 37 °C.

2.3. MTT assay

MTT assay was conducted according to manufacturer's instructions (Abcam, Cambridge, UK). In brief, MCF-10A cells were initially plated into a 6 cm culture dish. When reaching 90% confluence, the cells were harvested by trypsin digestion at 37 °C for 15 min. Then trypsin inhibitor was added 1:1 (*v*:*v*) to stop the digestion. Cells were pelleted by centrifugation at 1000 rpm for 5 min and then resuspended in fresh medium to reach a concentration of 5×10^4 cells/mL. A total of 5×10^3 cells (100 μL) were seeded into a 96-well plate for further incubation of 48 h. The medium in the 96-well plate was then replaced by the medium containing 10 μM, 5 μM, 2 μM, 1 μM, 500 nM, 200 nM, 100 nM, 10 nM, 1 nM of BPS. Medium containing 0.1% DMSO was used as control. Six duplicates were prepared for each concentration. After cultured for another 24 h, the medium was removed and 100 μL of fresh medium as well as 10 μL of MTT solution (5 mg/mL in PBS) were added to each well and incubated in 37 °C for another 4 h. Then 100 μL of SDS-HCl solution (1 g of SDS dissolved in 10 mL of 0.01 M HCl) was added to each well. The plate was incubated in 37 °C humidified chamber for 4 h to dissolve the purple formazan. Absorbance at 570 nm was measured.

2.4. Cell treatment for metabolomics and proteomics analysis

A total of 4×10^5 cells were initially plated in 6 cm culture dishes. When reaching 50% confluence, medium was changed to include 1 μM of BPS and 0.1% DMSO. Medium containing 0.1% DMSO was used as vehicle control. Then, cells were cultured in BPS-contained medium for another 24 h. Six duplicates were prepared for each group. Cells were harvested for the following experiments.

2.5. Metabolomics analysis

Metabolites were extracted from the control and 1 μM BPS treated MCF-10A cells for metabolomics study. The cell pellets were quenched by 600 μL of ice-cold 80% methanol/H_2O solution. Three repetitive freeze-thaw cycles with liquid nitrogen were conducted for cell lysis. Samples were then centrifuged at 15,000*g* for 10 min at 4 °C. The supernatants were collected, vacuum-dried and then redissolved in 50% methanol/H_2O containing 1 μg/mL of 4-Cl-Phe as the internal standard (IS). Samples were vortexed for 3 min and then centrifuged at 16,000*g* for 8 min at 4 °C. The supernatants were collected and subjected to LC-MS analysis. Quality control (QC) samples were prepared by pooling 40 μL of each sample.

LC-MS-based metabolic profiling was conducted on a LC-Q Exactive Focus Hybrid Quadrupole-Orbitrap MS as previously reported (Wei et al., 2018). To achieve relatively more comprehensive results, the samples were analyzed under both negative and positive ionization modes. Ten microliters of each sample were injected for analysis.

2.6. Quantitative proteomics analysis

Cells were treated with the lysis buffer containing 4% SDS, 20 mM Tris and protease inhibitor under sonication. Supernatants were collected by centrifugation of the samples at 14,000*g* for 10 min at 4 °C. Five volumes of ice-cold acetone was then added to each sample for protein precipitation at −20 °C overnight. The protein pellets were resuspended, and the concentrations were measured by Pierce™ BCA protein assay kit (Thermo Scientific, USA) according to the manufacturer's protocol. Afterwards, 100 μg of each sample was subjected to trypsin digestion following FASP protocol on a 30 KD filter (Millipore, Billerica, USA) as previously reported (Wiśniewski, 2016). The released peptides were collected and dried by a freeze-drier (Labconco, Kansas City, MO, USA). The peptides were then redissolved in 10 μL of 50 mM triethylammonium bicarbonate buffer. Four samples in each group and 20 μg of each sample were subjected to the labeling by the 8-plex iTRAQ reagents (Applied Biosystem Inc., CA, USA) according to manufacturer's protocol. The labeled samples were combined and subjected to fractionation. The eluates from each fraction were dried by the Max-Up (NB-504CIR) IR vacuum concentrator and then resuspended in 8 μL of 0.1% FA and 1 μL of each sample was subjected to nano-LC orbitrap MS analysis as previously reported (Ji et al., 2019). Three replicates of each sample were analyzed.

2.7. Data processing and statistical analysis

SIEVE software (Thermo Fisher Scientific, USA) was used for peak extraction and alignment of the metabolic profiling data. The normalized peak area was subjected to orthogonal partial least squares discriminant analysis (OPLS-DA) by using the SIMCA-P V13 software (Umetrics, Umea, Sweden). Adjusted *P* value and fold change (FC) were calculated according to the normalized peak area. The volcano plots were constructed by plotting the negative log of the *P* value on the vertical axis (base 10) versus the log of the FC (base 2) on the horizontal axis. The ion with a P value < 0.05 and FC > 1.2 was considered to be the potential significantly varied metabolite. The screened peaks were further identified by MS^2 fragments according to METLIN Database (https://metlin.scripps.edu/index.php) and the Human Metabolome Database (http://www.hmdb.ca/). The identified metabolites were then subjected to pathway analysis with MetaboAnalyst 3.0 (http://mirror.metaboanalyst.ca/) and mapped into pathways as illustrated in the Kyoto Encyclopedia of Genes and Genomes (KEGG) (https://www.genome.jp/kegg/).

For the iTRAQ proteomic data, the collected MS spectra were searched according to the UniProt-Swissport Human Database by the Mascot Daemon search engine. Proteins with FC > 1.5 and adjusted $P < 0.05$ were considered to be significantly differential expressed proteins (DEPs). Bioinformatics analyses of these DEPs were performed according to Gene Ontology (GO) annotation. Protein-protein interaction (PPI) network of the DEPs was performed using the online system String (https://string-db.org) with the highest interaction confidence of 0.90 and visualized with Cytoscape software (Shannon et al., 2003). The KEGG pathway analysis and GO ontology analysis of the DEPs were also run with String.

3. Results

3.1. BPS exposure altered the proliferation of MCF-10A cells in a hormetic manner

To assess the effects of BPS exposure on the growth of MCF-10A cells, MTT assay was conducted. As shown in Fig. 1, an inverted U-shape was observed in the MTT results, suggesting that BPS treatment altered the proliferation of MCF-10A cells in a hermetic manner. In the concentration range of 1 nM to 1 μM, the proliferation of MCF-10A cells was significantly increased with the increase of the concentrations. The highest proliferation rate was achieved by 1 μM and 2 μM of BPS exposure. While at concentrations higher than 2 μM, the proliferation rate showed a decreased tendency, possibly due to the cytotoxic effect at relatively high dosages of BPS exposure. These results indicated that low dose of BPS exposure significantly promoted the proliferation of MCF-10A cells.

3.2. Proteomics analysis

To better understand the changes and mechanisms involved in the effects of BPS on MCF-10A cells, global protein changes in BPS-treated cells were analyzed by iTRAQ method. The treatment dosage was 1 μM at which BPS exerted the maximum proliferation-promoting effects. In total, over 1500 proteins were identified and quantified. Among these proteins, 200 proteins were found to be significantly changed in the BPS exposure group (FC > 1.5, adjusted $P < 0.05$) (Table S1). According to the functional annotation, we found that several

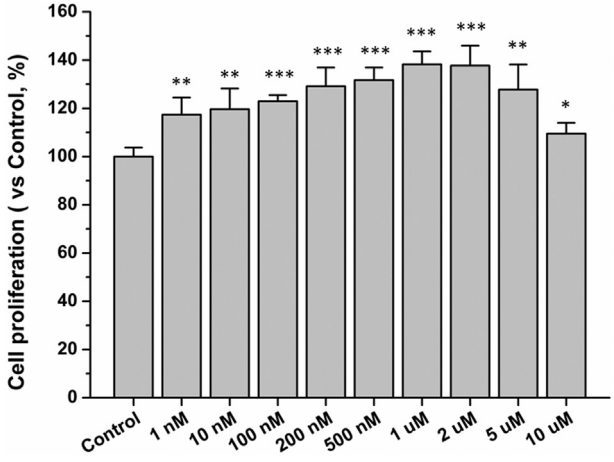

Fig. 1. MTT assay results for BPS exposure of MCF-10A cells at different concentrations. Results were analyzed in comparison with the control group by the Student's *t*-test. Data are shown as mean ± SEM (n = 6). *$P < 0.05$; **$P < 0.01$; ***$P < 0.001$.

of these DEPs were involved in cell proliferation, including the proliferation marker protein Ki-67 (MKI67), cell growth-regulating nucleolar protein (LYAR), scribble protein (SCRIB), caveolin 1 (CAV1), cadherin-1 (CDH-1), SHC-transforming protein 1 (SHC1), high mobility group AT-hook 2 (HMGA2) (Fig. 2A and Table S1), further demonstrating the influence of BPS on proliferation of MCF-10A cells.

The PPI network of the DEPs was enriched in 222 interactions with a P value $< 1 \times 10^{-6}$. The DEPs were grouped into 15 clusters with at least 2 nodes (Fig. S1). This PPI network suggested that these DEPs interact strongly with and contribute to numerous biological processes. The GO terms for biological process, KEGG pathways and reactome pathways were obtained for the DEPs. According to the biological process classification, these DEPs were involved in a wide range of biological processes which were related to cellular metabolic, mitochondrial gene expression, cellular respiration, mitochondrion organization, modification of morphology or physiology of organism, ribosome biogenesis, transmembrane transporter activity (Fig. 3A and Table S2). As for the reactome pathways, the DEPs were involved in biological reactions related to mitochondrial translation, the citric acid (TCA) cycle and respiratory electron transport, pre-mRNA processing, EGFR signaling and rRNA modification (Fig. 3B). With respect to KEGG pathways, there is a substantial enrichment in oxidative phosphorylation (FDR = 0.00031) (Fig. 3C). These results suggested that the mitochondrial function, gene expression, energy metabolism and signaling transduction were altered in MCF-10A cells in response to low dose of BPS exposure.

Among the DEP clusters, a cluster with the hub protein of EGFR was observed (Fig. S1). Besides, the expression levels of EGFR, ragulator complex protein LAMTOR1, and several Ras-related proteins were increased in BPS-exposed group (Fig. 2B and Table S1). Along with this point, the terms of "constitutive signaling by EGFR" and "Ras protein signal transduction" were observed to be of significance (Fig. 3A and B). These results suggested the involvement of EGFR and related signaling pathways in BPS-induced proliferation of MCF-10A cells. What's more, we noticed that several proteins related to cellular apoptosis were clustered and significantly downregulated by BPS exposure, including BAK1 (Bcl-2 Homologous Antagonist Killer 1), DIABLO (Second Mitochondria-derived Activator of Caspases), CYC1 (Cytochrome c1) and QCR9 (cytochrome b-c1 complex subunit 9) (Figs. 2C and S1).

3.3. Metabolomics analysis

To further assess changes in the downstream metabolic pathways in response to BPS exposure, endogenous metabolites were analyzed by LC-MS-based metabolic profiling under both negative and positive ionization modes. The OPLS-DA scores plots showed obvious separation between BPS exposure group and control group in both negative (Fig. S2A) and positive (Fig. S2B) ionization mode, which were described by high values of R^2X (0.682 and 0.866), R^2Y (0.996 and 1) and Q^2 (0.518 and 0.652) parameters, indicating powerful and reliable models. Volcano plots were drawn with P value and FC of all the extracted ions. As shown in Fig. S2C and D, potential upregulated and downregulated metabolites were marked in red dots and blue dots, respectively (FC > 1.2, $P < 0.05$). By further MS^2 identification, 35 significantly changed ions were matched with endogenous metabolites from HMDB database (Table S3). As shown in Fig. 4A and Table S3, 20 of the identified metabolites were downregulated and 15 were upregulated by BPS exposure. Metabolite set enrichment analysis (MSEA) against the Small Molecule Pathway Database (SMPDB) showed that these differential metabolites were enriched in a wide range of pathways. Among these pathways, the glutamate metabolism, purine metabolism and Warburg effect had the P values < 0.05 and enrichment factors larger than 3 (Fig. S3). Further pathway topology analysis showed that the most targeted pathways were purine metabolism, TCA cycle, phenylalanine metabolism, alanine, aspartate and glutamate metabolism, glycerophospholipid metabolism, pyruvate metabolism (Fig. 4B). These results showed the dramatic metabolic remodeling induced by BPS in MCF-10A cells.

3.4. Integrated proteomics and metabolomics analysis

As we know, most enzymes that participate in metabolic processes are proteins. To associate the proteomics data with the metabolomics data, we conducted a joint pathway analysis with the DEPs and

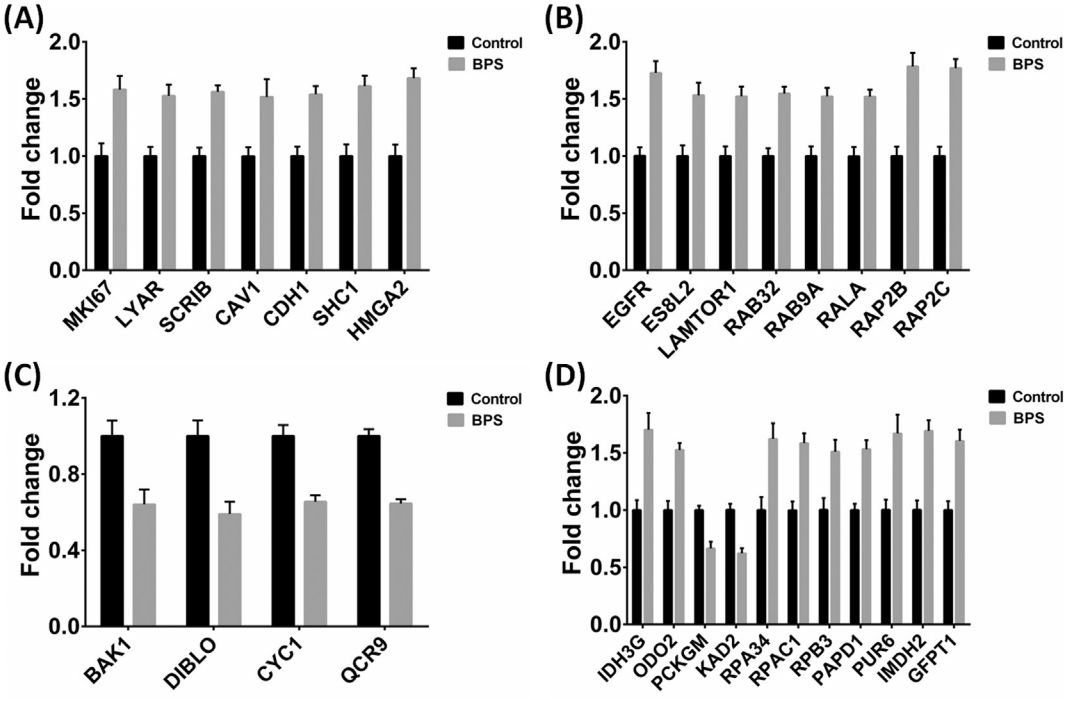

Fig. 2. Representative DEPs identified by iTRAQ-based proteomics, which were related to (A) cell proliferation, (B) EGFR signaling, (C) apoptosis, (D) metabolic pathways including TCA cycle, pyruvate metabolism, purine metabolism and glutamate metabolism.

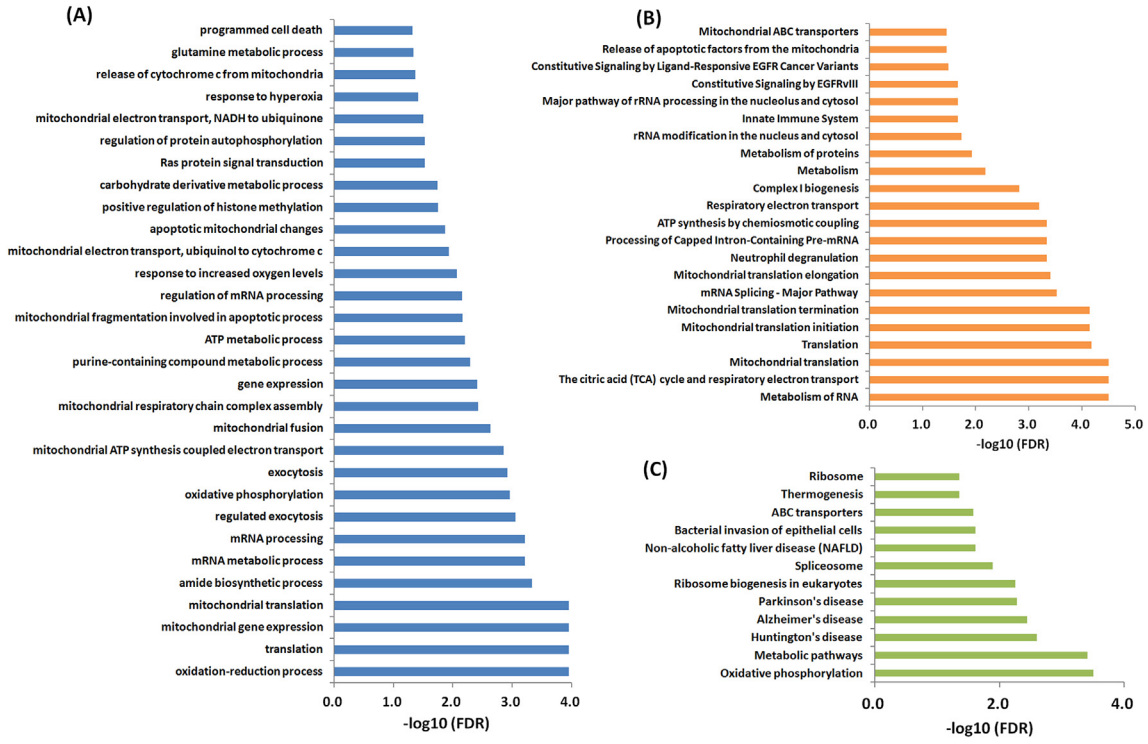

Fig. 3. Bioinformatics analysis of the DEPs by String (https://string-db.org): (A) Representative biological processes; (B) Reactome pathways; (C) KEGG pathways.

differential metabolites. The results revealed that several metabolic pathways were significantly targeted, including TCA cycle, purine metabolism, glycosylphosphatidylinositol (GPI)-anchor biosynthesis, pyruvate metabolism and alanine, aspartate and glutamate metabolism (Fig. 5), further relating these pathways to BPS exposure-induced effects on MCF-10A cells. As shown in Figs. 2D and 6, the increase of downstream metabolite malate and decrease of succinate as well as the increased expression of involved proteins (IDH3G, ODO2) suggested the upregulation of TCA cycle by BPS exposure. Besides, increased phosphoenol pyruvate and D-glycerate-3-phosphate which were derived from glycolysis, and decreased phosphoenolpyruvate carboxykinase [GTP] protein (PCKGM) indicated the increase in glycolysis and pyruvate metabolism. In purine metabolism pathway, we observed the decrease of hypoxanthine, guanine and inosine, which are the downstream metabolites. At the same time, we found the increase of adenosine monophosphate (AMP), adenosine diphosphate ribose, guanosine monophosphate (GMP) and the inosine-5′-monophosphate dehydrogenase 2 (IMDH2), suggesting the inhibition of purine degradation. In addition, the increased expression of multifunctional protein ADE2 (PUR6) suggested the upregulation of de novo purine biosynthesis. Finally, glutamate metabolism pathway was shown to be upregulated by BPS exposure as decrease of glutamate and upregulation of glutamine-fructose-6-phosphate aminotransferase1 (GFTP1) were observed.

4. Discussion

As the usage of BPS is not regulated, human is widely exposed to this emerging contaminant in daily life (Wu et al., 2018). The median estimated daily intake of BPS from several studies was below the reference

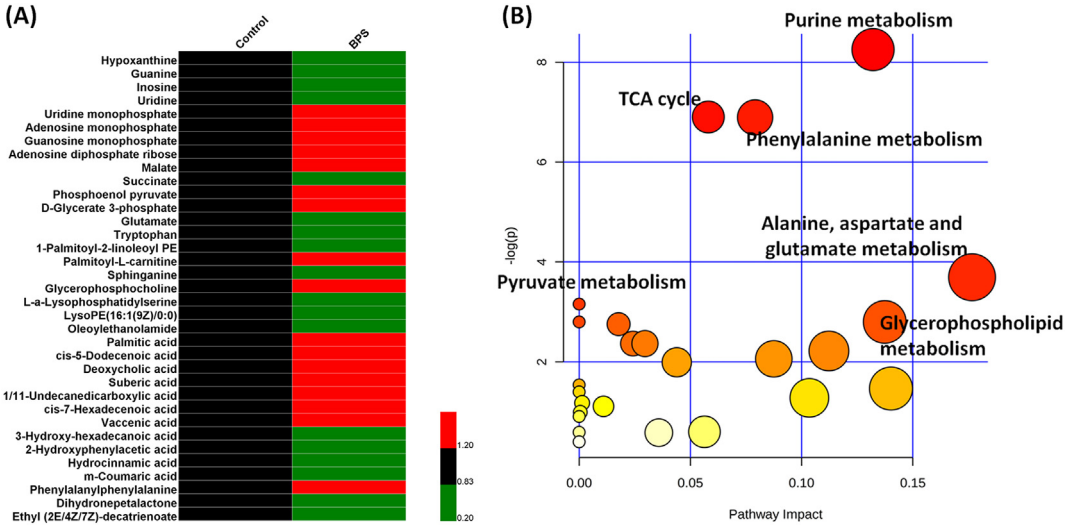

Fig. 4. Metabolic disturbances in BPS-exposed MCF-10A cells: (A) Differential metabolites identified by LC-MS; (B) Topology pathway analysis with the altered metabolites.

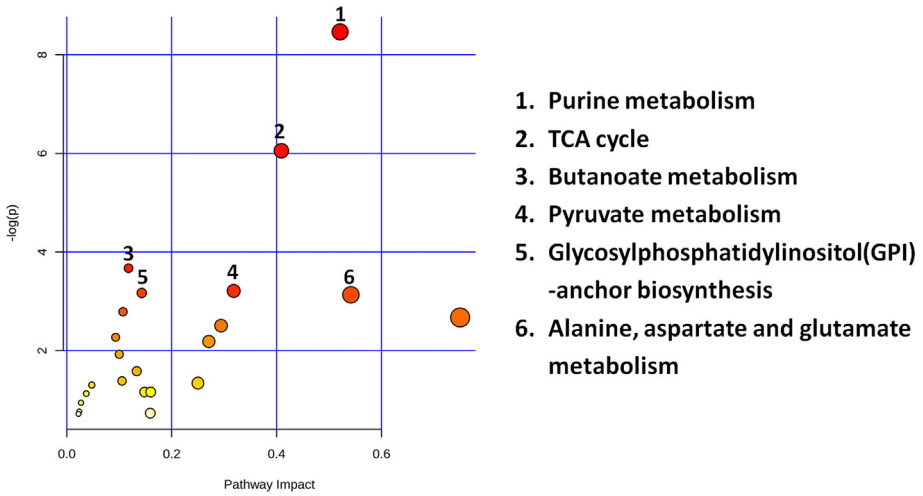

Fig. 5. Joint pathway analysis of the DEPs and differential metabolites by metabolite-centric pathway analysis. The labeled pathways were of *P* values < 0.05.

dose set for BPA by several environmental organizations, suggesting a relatively low internal exposure level of BPS in general populations (Liao et al., 2012b; Chen et al., 2018a,b). Although BPS has been reported to have the similar estrogenic effect as BPA and could induce the proliferation of ER positive breast cells (Rochester and Bolden, 2015), the influence of low dose of BPS exposure on ER negative cells, especially normal cells, has not been fully elucidated. The human breast epithelial cell line MCF-10A is ER negative cells, retaining many of the characteristics of normal breast epithelium (Lane et al., 1999). As MCF-10A cell is immortalized and not tumorigenic, it has been used in many breast cancer studies as the step of early changes on the scale of tumorigenic transformation (Balani et al., 2017). We showed here that BPS could alter the proliferation of MCF-10A cells in a hormetic manner. Hormesis is generally characterized by low dose stimulation and high dose inhibition. In present study, we focused mainly on the effects induced by low dose of BPS exposure because of its relatively low

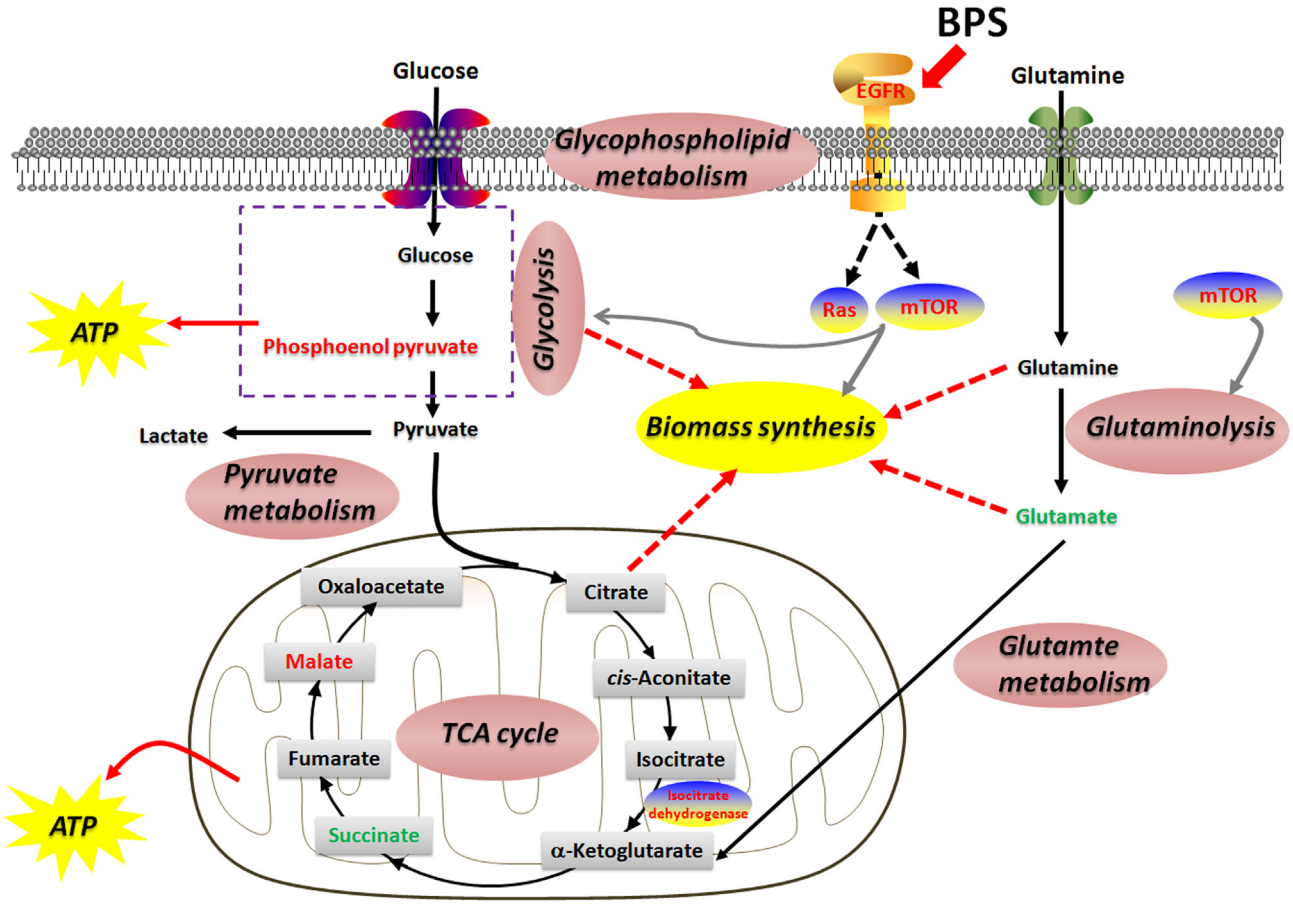

Fig. 6. Proposed signaling and metabolic pathways for BPS-induced promotion of proliferation in MCF-10A cells. Increased metabolites and proteins were labeled in red, decreased ones were in green, and black ones were unchanged or not detected in current work. (For interpretation of the references to colour in this figure legend, the reader is referred to the web version of this article.)

environmental and human exposure levels (Wu et al., 2018). Significant promotion of proliferation was observed in MCF-10A cells by exposure of low concentrations of BPS. This result is akin to previous findings that BPA at low, noncytotoxic levels could regulate non-estrogenic proliferation in ER negative cells including MCF-10A, demonstrating a possibly similar ER-independent mechanism through which BPS acts on mammary cells.

The stimulation effect of low concentrations might result in the loss of regulation and equilibrium of cell functions, especially in view of development. Previous reports showed that hormetic response was mediated through receptor and/or signaling pathways (Calabrese, 2013). The proteomics results of this study suggested that upregulation of EGFR and EGFR-transducted signaling pathways were involved in acceleration of proliferation by low dose of BPS exposure. EGFR has been reported to mediate epithelial cell proliferation. Two important pathways in mediating the biological response of EGFR were RAS-RAF-MEK-MAPK pathway and PI3K-AKT-mTOR pathway (Wee and Wang, 2017). Activation of EGFR is related to tyrosine phosphorylation, which was possibly associated with oxidative stress. Many reactive oxygen species (ROS)-producing chemicals have been reported to activate EGFR signaling pathway in cells (Weng et al., 2018). In ER negative breast cells, BPA exerts its proliferative effect through activation of EGFR signaling pathway (Sauer et al., 2017). Besides, exposure of MCF-10A cell line to 2,3,7,8-tetrachlorodibenzo-*p*-dioxin (TCDD) has been reported to mediate increase in cell number and inhibition of apoptosis via the EGFR pathway (Davis et al., 2001). Benzo(a)pyrene quinones could induce the EGFR cell signaling and activate genes associated with cell proliferation in MCF-10A cells (Burdick et al., 2003). In addition, ethanol exposure increased oxidative stress and EGFR tyrosine phosphorylation in MCF-10A cells overexpressing CYP2E1 (León-Buitimea et al., 2012). Taken these findings and our results into consideration, we believed that low dose of BPS exposure upregulated the EGFR signaling and downstream Ras and mTOR-related signaling pathways, further exerting effects on metabolic pathways to sustain the proliferation in MCF-10A cells.

In addition to promoting cell proliferation, several markers of cell apoptosis were also changed by BPS exposure. The Bcl-2 family of proteins governs mitochondrial membrane permeability to regulate the release of cytochrome *c* from the mitochondria (Shimizu et al., 1999). BAK1 has been annotated to be one of the pro-apoptotic proteins in Bcl-2 family of proteins (Kuwana and Newmeyer, 2003). DIABLO has been reported to promote apoptosis by inhibiting activity of inhibitors of apoptosis proteins (Fu et al., 2003). Moreover, biological terms of "apoptotic mitochondrial changes", "release of cytochrome c from the mitochondria" and "programmed cell death" were shown to be significantly enriched. The down regulation of these proteins and pathways implicated that BPS exposure might inhibit the apoptosis of MCF-10A cells. However, to further confirm this, more cellular analyses about the apoptotic parameters would be needed in future studies.

Overwhelming evidences have shown that metabolic regulation influences cell proliferation. Increased energy production and macromolecule synthesis are necessary in proliferating cells (DeBerardinis et al., 2008). Cells use precursors derived from intermediates of TCA cycle and glutamate metabolism to synthesize lipids, proteins and nucleic acids for proliferation (Vander Heiden et al., 2011). TCA cycle has been reported to be the central oxidative phosphorylation route in cells, acting as the hub for energy metabolism, macromolecule synthesis and redox balance (Anderson et al., 2018). Besides, proliferating cells have been proved to show significant increase in glutamate utilization by catabolizing more glutamate via transaminases to couple non-essential amino acid synthesis to α-ketoglutarate generation and TCA cycle anaplerosis (Coloff et al., 2016). Therefore, we speculated that the upregulation of TCA cycle and glutamate metabolism in BPS-exposed MCF-10A cells would supply the increased demand of energy and biosynthetic substrates for proliferation.

Purines and pyrimidines provide essential components for nucleic acids. Previous report showed that in dividing cells, the de novo biosynthetic pathway is fundamental to replenish the purine pool (Lane and Fan, 2015). Purines have been reported to regulate the cell cycle progression in T lymphocytes (Quéméneur et al., 2003). Except for acting as the biosynthetic precursors, purine containing metabolites could also act as signaling molecules, such as adenosine, AMP, ATP (Hardie et al., 2016). Purine nucleotides could activate the mechanistic target of rapamycin complex 1 (mTORC1) pathway, which promotes the anabolic conversion of nutrients into macromolecules (Ben-Sahra et al., 2016). So, it remains possible that the increased purine-containing metabolites may regulate the mTOR signaling, further promoting the biosynthetic processes.

Our results also suggested that BPS exposure caused disturbance in glycerophospholipid metabolism and GPI-anchor biosynthesis. Lipids are key molecular integrators of membrane structure and dynamics, energy homeostasis, and signaling. Both the glycerophospholipid and GPI-anchor are important components of membrane. Lipids environment of the membrane could influence the folding, structure and function of membrane proteins (Laganowsky et al., 2014). Changes in glycerophospholipids might affect membrane curvature and thereby influence membrane fusion, fission and vesicle transport (McMahon and Boucrot, 2015). Previous report has also demonstrated that lipid composition in membrane exerts a profound regulatory effect on kinase domain activation of the EGFR (Coskun et al., 2011). We inferred that the alterations of these lipid-related pathways induced by BPS exposure might also play a role in EGFR signaling transduction.

Collectively, we proposed the possible pathways through which BPS acts on the ER negative breast epithelial cells MCF-10A based on our findings and previous reports. As shown in Fig. 6, BPS exposure upregulated the EGFR and the EGFR signaling transduction, which would lead to the upregulation of downstream signaling pathways with involvement of Ras and mTOR. Along with these pathways, cellular metabolic pathways including glycolysis, pyruvate metabolism, glutamate metabolism and TCA cycle were upregulated to enable the cell to obtain energy and substrates for anabolic building block production for cell proliferation.

5. Conclusions

In the current work, we assessed the effects of BPS on normal ER negative breast epithelial MCF-10A cells. Promotion of proliferation by low dose of BPS was observed in the targeted cell line. By using the integration of iTRAQ-based proteomics and non-targeted metabolomics, we further yield additional insights into the pathways that might be responsible for cell proliferation, exemplifying the strength of multi-omics approaches. Our results implied the influence of low concentrations of BPS on normal breast cells and further broadened our knowledge on the biological effects of BPS. Additional studies are needed to fully demonstrate the whole signaling transduction pathways, by which BPS regulates the growth of human mammary cells.

Declaration of competing interest

The authors declare that they have no known competing financial interests or personal relationships that could have appeared to influence the work reported in this paper.

Acknowledgement

This work was supported by National Natural Science Foundation of China (91543202, 21806135, 21705137 and 21507106), Hong Kong Research Grants Council-General Research Fund (1230195), Hong Kong Baptist University Strategic Development Fund (15-1012-P04), Hong Kong Scholars Program Fund (XJ2016010). Dr.

Simon Wang at the Language Centre, Hong Kong Baptist University, has helped improve the linguistic presentation of this manuscript.

Appendix A. Supplementary data

Supplementary data to this article can be found online at https://doi.org/10.1016/j.scitotenv.2019.136453.

References

Aebersold, R., Mann, M., 2016. Mass-spectrometric exploration of proteome structure and function. Nature 537 (7620), 347.

Anderson, N.M., et al., 2018. The emerging role and targetability of the TCA cycle in cancer metabolism. Protein Cell 9 (2), 216–237.

Ayyanan, A., et al., 2011. Perinatal exposure to bisphenol a increases adult mammary gland progesterone response and cell number. Mol. Endocrinol. 25 (11), 1915–1923.

Balani, S., et al., 2017. Modeling the process of human tumorigenesis. Nat. Commun. 8, 15422.

Ben-Sahra, I., et al., 2016. mTORC1 induces purine synthesis through control of the mitochondrial tetrahydrofolate cycle. Science 351 (6274), 728.

Burdick, A.D., et al., 2003. Benzo (a) pyrene quinones increase cell proliferation, generate reactive oxygen species, and transactivate the epidermal growth factor receptor in breast epithelial cells. Cancer Res. 63 (22), 7825–7833.

Calabrese, E.J., 2013. Hormetic mechanisms. Crit. Rev. Toxicol. 43 (7), 580–606.

Chen, D., et al., 2016. Bisphenol analogues other than BPA: environmental occurrence, human exposure, and toxicity–a review. Environ. Sci. Technol. 50 (11), 5438–5453.

Chen, H., et al., 2018a. An integrated metabolomic and proteomic study of toxic effects of Benzo[a]pyrene on gills of the pearl oyster Pinctada martensii. Ecotoxicol. Environ. Saf. 156, 330–336.

Chen, Y., et al., 2018b. Urinary bisphenol analogues and triclosan in children from south China and implications for human exposure. Environ. Pollut. 238, 299–305.

Coloff, J.L., et al., 2016. Differential glutamate metabolism in proliferating and quiescent mammary epithelial cells. Cell Metab. 23 (5), 867–880.

Commission, E., 2011. Bisphenol A: EU Ban on Baby Bottles to Enter Into Force Tomorrow.

Coskun, Ü., et al., 2011. Regulation of human EGF receptor by lipids. Proc. Natl. Acad. Sci. 108 (22), 9044.

Davis, J.W., et al., 2001. Prevention of apoptosis by 2, 3, 7, 8-tetrachlorodibenzo-p-dioxin (TCDD) in the MCF-10A cell line: correlation with increased transforming growth factor α production. Cancer Res. 61 (8), 3314–3320.

DeBerardinis, R.J., et al., 2008. The biology of cancer: metabolic reprogramming fuels cell growth and proliferation. Cell Metab. 7 (1), 11–20.

Deng, Q.Q., et al., 2018. GPER/Hippo-YAP signal is involved in Bisphenol S induced migration of triple negative breast cancer (TNBC) cells. J. Hazard. Mater. 355, 1–9.

Fu, J., et al., 2003. Smac3, a novel Smac/DIABLO splicing variant, attenuates the stability and apoptosis-inhibiting activity of X-linked inhibitor of apoptosis protein. J. Biol. Chem. 278 (52), 52660–52672.

Gioria, S., et al., 2016. A combined proteomics and metabolomics approach to assess the effects of gold nanoparticles in vitro. Nanotoxicology 10 (6), 736–748.

Go, Y.-M., et al., 2014. Integrated redox proteomics and metabolomics of mitochondria to identify mechanisms of Cd toxicity. Toxicol. Sci. 139 (1), 59–73.

Gowda, G.N., et al., 2008. Metabolomics-based methods for early disease diagnostics. Expert. Rev. Mol. Diagn. 8 (5), 617–633.

Gstaiger, M., Aebersold, R., 2009. Applying mass spectrometry-based proteomics to genetics, genomics and network biology. Nat. Rev. Genet. 10 (9), 617.

Hardie, D.G., et al., 2016. AMPK: an energy-sensing pathway with multiple inputs and outputs. Trends Cell Biol. 26 (3), 190–201.

Huang, W., et al., 2019. Bisphenol S induced epigenetic and transcriptional changes in human breast cancer cell line MCF-7. Environ. Pollut. 246, 697–703.

Jalal, N., et al., 2018. Bisphenol A (BPA) the mighty and the mutagenic. Toxicol. Rep. 5, 76–84.

Ji, C., et al., 2013. Proteomic and metabolomic analysis of earthworm Eisenia fetida exposed to different concentrations of 2,2′,4,4′-tetrabromodiphenyl ether. J. Proteome 91, 405–416.

Ji, C., et al., 2016. An integrated proteomic and metabolomic study on the gender-specific responses of mussels Mytilus galloprovincialis to tetrabromobisphenol A (TBBPA). Chemosphere 144, 527–539.

Ji, F., et al., 2019. Study of BDE-47 induced Parkinson's disease-like metabolic changes in C57BL/6 mice by integrated metabolomic, lipidomic and proteomic analysis. J. Hazard. Mater. 378, 120738.

Kolla, S., et al., 2018. Low dose bisphenol S or ethinyl estradiol exposures during the perinatal period alter female mouse mammary gland development. Reprod. Toxicol. 78, 50–59.

Kuwana, T., Newmeyer, D.D., 2003. Bcl-2-family proteins and the role of mitochondria in apoptosis. Curr. Opin. Cell Biol. 15 (6), 691–699.

Laganowsky, A., et al., 2014. Membrane proteins bind lipids selectively to modulate their structure and function. Nature 510, 172.

Lane, A.N., Fan, T.W.-M., 2015. Regulation of mammalian nucleotide metabolism and biosynthesis. Nucleic Acids Res. 43 (4), 2466–2485.

Lane, M., et al., 1999. Spontaneous conversion to estrogen receptor expression by the human breast epithelial cell line, MCF-10A. Oncol. Rep. 6 (3), 507–518.

LaPlante, C.D., et al., 2017. Bisphenol S alters the lactating mammary gland and nursing behaviors in mice exposed during pregnancy and lactation. Endocrinology 158 (10), 3448–3461.

León-Buitimea, A., et al., 2012. Ethanol-induced oxidative stress is associated with EGF receptor phosphorylation in MCF-10A cells overexpressing CYP2E1. Toxicol. Lett. 209 (2), 161–165.

Liao, C., et al., 2012a. Bisphenol S in urine from the United States and seven Asian countries: occurrence and human exposures. Environ. Sci. Technol. 46 (12), 6860–6866.

Liao, C., et al., 2012b. Bisphenol s, a new bisphenol analogue, in paper products and currency bills and its association with bisphenol a residues. Environ. Sci. Technol. 46 (12), 6515–6522.

Lin, Z.X., et al., 2019. Bisphenol S promotes the cell cycle progression and cell proliferation through ER alpha-cyclin D-CDK4/6-pRb pathway in MCF-7 breast cancer cells. Toxicol. Appl. Pharmacol. 366, 75–82.

Mandrup, K., et al., 2016. Low-dose effects of bisphenol A on mammary gland development in rats. Andrology 4 (4), 673–683.

McMahon, H.T., Boucrot, E., 2015. Membrane curvature at a glance. J. Cell Sci. 128 (6), 1065–1070.

Pfeifer, D., et al., 2015. Effects of low-dose bisphenol A on DNA damage and proliferation of breast cells: the role of c-Myc. Environ. Health Perspect. 123 (12), 1271–1279.

Pupo, M., et al., 2012. Bisphenol A induces gene expression changes and proliferative effects through GPER in breast cancer cells and cancer-associated fibroblasts. Environ. Health Perspect. 120 (8), 1177–1182.

Quéméneur, L., et al., 2003. Differential control of cell cycle, proliferation, and survival of primary T lymphocytes by purine and pyrimidine nucleotides. J. Immunol. 170 (10), 4986.

Rezg, R., et al., 2014. Bisphenol A and human chronic diseases: current evidences, possible mechanisms, and future perspectives. Environ. Int. 64, 83–90.

Rochester, J.R., Bolden, A.L., 2015. Bisphenol S and F: a systematic review and comparison of the hormonal activity of bisphenol A substitutes. Environ. Health Perspect. 123 (7), 643–650.

Saji, S., et al., 2000. Estrogen receptors alpha and beta in the rodent mammary gland. Proc. Natl. Acad. Sci. U. S. A. 97 (1), 337–342.

Samuelsen, M., et al., 2001. Estrogen-like properties of brominated analogs of bisphenol A in the MCF-7 human breast cancer cell line. Cell Biol. Toxicol. 17 (3), 139–151.

Sauer, S.J., et al., 2017. Bisphenol A activates EGFR and ERK promoting proliferation, tumor spheroid formation and resistance to EGFR pathway inhibition in estrogen receptor-negative inflammatory breast cancer cells. Carcinogenesis 38 (3), 252–260.

Shannon, P., et al., 2003. Cytoscape: a software environment for integrated models of biomolecular interaction networks. Genome Res. 13 (11), 2498–2504.

Shimizu, S., et al., 1999. Bcl-2 family proteins regulate the release of apoptogenic cytochrome c by the mitochondrial channel VDAC. Nature 399 (6735), 483.

Song, Q., et al., 2017. Toxic responses of Perna viridis hepatopancreas exposed to DDT, benzo(a)pyrene and their mixture uncovered by iTRAQ-based proteomics and NMR-based metabolomics. Aquat. Toxicol. 192, 48–57.

Soule, H.D., et al., 1990. Isolation and characterization of a spontaneously immortalized human breast epithelial cell line, MCF-10. Cancer Res. 50 (18), 6075.

Tucker, D.K., et al., 2018. Evaluation of prenatal exposure to bisphenol analogues on development and long-term health of the mammary gland in female mice. Environ. Health Perspect. 126 (8), 087003.

Vander Heiden, M., et al., 2011. Metabolic pathway alterations that support cell proliferation. Cold Spring Harb Sym. Cold Spring Harbor Laboratory Press.

Wang, Z., et al., 2017. Low-dose bisphenol A exposure: a seemingly instigating carcinogenic effect on breast cancer. Adv. Sci. 4 (2), 1600248.

Wee, P., Wang, Z., 2017. Epidermal growth factor receptor cell proliferation signaling pathways. Cancers 9 (5), 52.

Wei, J., et al., 2018. Metabolic profiling on the effect of 2,2′,4,4′-tetrabromodiphenyl ether (BDE-47) in MCF-7 cells. Chemosphere 192, 297–304.

Weng, M.-S., et al., 2018. The interplay of reactive oxygen species and the epidermal growth factor receptor in tumor progression and drug resistance. J. Exp. Clin. Cancer Res. 37 (1), 61.

Williams, G.P., Darbre, P.D., 2019. Low-dose environmental endocrine disruptors, increase aromatase activity, estradiol biosynthesis and cell proliferation in human breast cells. Mol. Cell. Endocrinol. 486, 55–64.

Wiśniewski, J.R., 2016. Quantitative evaluation of filter aided sample preparation (FASP) and multienzyme digestion FASP protocols. Anal. Chem. 88 (10), 5438–5443.

Wu, L.-H., et al., 2018. Occurrence of bisphenol S in the environment and implications for human exposure: a short review. Sci. Total Environ. 615, 87–98.

Xie, J., et al., 2018. Research on the hepatotoxicity mechanism of citrate-modified silver nanoparticles based on metabolomics and proteomics. Nanotoxicology 12 (1), 18–31.

Zhang, A., et al., 2016. Mass spectrometry-based metabolomics: applications to biomarker and metabolic pathway research. Biomed. Chromatogr. 30 (1), 7–12.

Zientek-Targosz, H., et al., 2008. Transformation of MCF-10A cells by random mutagenesis with frameshift mutagen ICR191: a model for identifying candidate breast-tumor suppressors. Mol. Cancer 7, 51.